Article

Cell Reports

Voluntary Running Triggers VGF-Mediated Oligodendrogenesis to Prolong the Lifespan of Snf2h-Null Ataxic Mice

Graphical Abstract

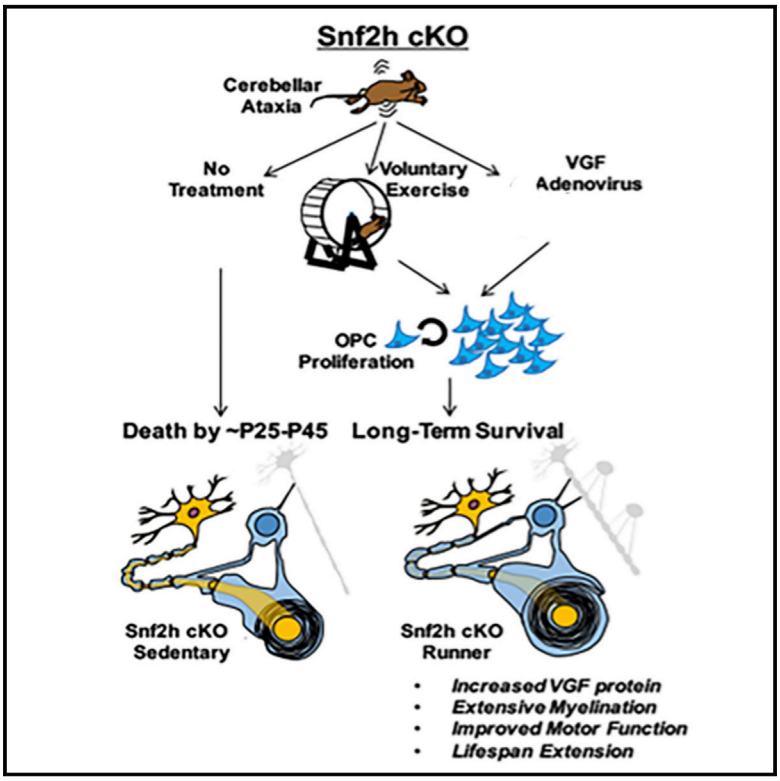

Highlights

- Running promotes the survival of mice with cerebellar ataxia following *Snf2h* inactivation
- Running ataxic mice show enhanced oligodendrogenesis and de novo myelination
- Comparative RNA-seq studies identify VGF as a contributor to brain repair
- VGF overexpression improves ataxic phenotype in mice without exercise

Authors

Matías Alvarez-Saavedra, Yves De Repentigny, Doo Yang, ..., Robin J. Parks, Rashmi Kothary, David J. Picketts

Correspondence

matias.alvarez-saavedra@nyumc.org (M.A.-S.), dpicketts@ohri.ca (D.J.P.)

In Brief

Alvarez-Saavedra et al. find that voluntary running induces expression of the VGF growth factor and improves the ataxic phenotype of *Snf2h* cKO mice. Surviving *Snf2h* cKO mice show enhanced oligodendrogenesis and myelination in the hindbrain that is not seen in sedentary *Snf2h* cKO or control mice. Adenoviral-mediated VGF overexpression can also improve motor deficits and prolong lifespan without exercise.

Accession Numbers

GSE86235

Alvarez-Saavedra et al., 2016, Cell Reports *17*, 862–875
October 11, 2016
http://dx.doi.org/10.1016/j.celrep.2016.09.030

OPEN ACCESS
CellPress

Cell Reports
Article

Voluntary Running Triggers VGF-Mediated Oligodendrogenesis to Prolong the Lifespan of Snf2h-Null Ataxic Mice

Matías Alvarez-Saavedra,[1,2,7,8,9,*] Yves De Repentigny,[1] Doo Yang,[3,4] Ryan W. O'Meara,[1,2] Keqin Yan,[1] Lukas E. Hashem,[1,2] Lemuel Racacho,[3,5] Ilya Ioshikhes,[3,4] Dennis E. Bulman,[5,6] Robin J. Parks,[1,3] Rashmi Kothary,[1,2] and David J. Picketts[1,2,3,*]

[1]Regenerative Medicine Program, Ottawa Hospital Research Institute, 501 Smyth Road, Ottawa, ON K1H 8L1, Canada
[2]Department of Cellular and Molecular Medicine, University of Ottawa, ON K1N 6N5, Canada
[3]Department of Biochemistry, Microbiology & Immunology, University of Ottawa, ON K1N 6N5, Canada
[4]Ottawa Institute of Systems Biology (OISB), University of Ottawa, ON K1N 6N5, Canada
[5]Children's Hospital of Eastern Ontario Research Institute, Ottawa, ON K1N 6N5, Canada
[6]Department of Pediatrics, University of Ottawa, Ottawa, ON K1N 6N5, Canada
[7]Center for Biomedical Research, Faculty of Biological Sciences, Universidad Andres Bello, Avenida República 239, Santiago, Chile
[8]Present address: Department of Biochemistry & Molecular Pharmacology, Smilow Research Center, Howard Hughes Medical Institute, NYU School of Medicine, 522 First Avenue, New York, NY 10016, USA
[9]Lead Contact
*Correspondence: matias.alvarez-saavedra@nyumc.org (M.A.-S.), dpicketts@ohri.ca (D.J.P.)
http://dx.doi.org/10.1016/j.celrep.2016.09.030

SUMMARY

Exercise has been argued to enhance cognitive function and slow progressive neurodegenerative disease. Although exercise promotes neurogenesis, oligodendrogenesis and adaptive myelination are also significant contributors to brain repair and brain health. Nonetheless, the molecular details underlying these effects remain poorly understood. Conditional ablation of the *Snf2h* gene impairs cerebellar development producing mice with poor motor function, progressive ataxia, and death between postnatal days 25–45. Here, we show that voluntary running induced an endogenous brain repair mechanism that resulted in a striking increase in hindbrain myelination and the long-term survival of *Snf2h* cKO mice. Further experiments identified the VGF growth factor as a major driver underlying this effect. VGF neuropeptides promote oligodendrogenesis in vitro, whereas *Snf2h* cKO mice treated with full-length VGF-encoding adenoviruses removed the requirement of exercise for survival. Together, these results suggest that VGF delivery could represent a therapeutic strategy for cerebellar ataxia and other pathologies of the CNS.

INTRODUCTION

Clinical studies show that physical exercise protects against brain atrophy and reduces the risk of dementia, as well as promoting cerebral and cardiovascular health (Barnes, 2015). The protective effect of exercise is also being recognized as a means to enhance cognitive function and slow down neurodegenerative disease progression and disability (Erickson et al., 2011; Pereira et al., 2007). Indeed, rodent studies have confirmed that exercise regimens improve motor and cognitive functions in a variety of neurodegenerative models including stroke, Parkinson's disease, Alzheimer's disease, spinocerebellar ataxia, and multiple sclerosis (Abbott et al., 2004; Colcombe et al., 2004; Cruise et al., 2011; Fryer et al., 2011; Heyn et al., 2004; Khalil et al., 2013; Verghese et al., 2003). Despite these advances, our understanding of the molecular mechanisms by which exercise impedes or protects from neurodegeneration remains poorly understood.

Physical exercise increases skeletal muscle metabolism by enhanced contractile and epinephrine activity that drive adaptive responses to alter whole body energy and glucose homeostasis. Among these responses is the secretion of autocrine and paracrine factors from the muscle, collectively called myokines. These include IL-6, IL-15, IGF-1, and brain-derived growth factor (BDNF), whose functions are to increase appetite, improve mood, increase mitochondrial oxidative phosphorylation, and enhance overall metabolic efficiency (Pedersen and Febbraio, 2012). Of these, BDNF has an impact on brain function with several studies demonstrating that exercise promotes the generation of new neurons within the hippocampus, improves memory, and improves performance in aged mice (van Praag et al., 1999a, 1999b, 2005). Similarly, the neuropeptide precursor VGF (non-acronymic; also known as nerve growth factor inducible; unrelated to VEGF) is also upregulated upon exercise and promotes an anti-depressant response (Hunsberger et al., 2007). Other studies suggest that VGF-processed peptides function to maintain BDNF expression in a VGF-BDNF-positive feedback loop (Alder et al., 2003; Bozdagi et al., 2008; Hunsberger et al., 2007). However, the

importance of VGF to delaying or preventing neurodegeneration remains obscure.

Although significant attention has focused on the idea that exercise promotes the activation of neurogenesis, recent papers suggest that oligodendrogenesis is also a significant contributor to brain repair and the maintenance of brain health. Recent studies have shown that neuronal activity promotes oligodendrogenesis and adaptive myelination in complex learning tasks or following demyelination injury (Brousse et al., 2015; Gautier et al., 2015; Gibson et al., 2014). Voluntary exercise also increased oligodendrogenesis in the spinal cord of nestin-GFP transgenic mice (Krityakiarana et al., 2010). Other studies show that injury results in massive recruitment of cells from the subventricular zone (SVZ) that adopt an oligodendrocytic fate, whereas another study showed that de novo synapse formation onto OPCs resulted in glutamate-induced differentiation of oligodendrocytes to facilitate remyelination (Brousse et al., 2015; Gautier et al., 2015). Similarly, Piao et al. (2015) demonstrated that engrafted OPCs derived from human ESCs could facilitate forebrain and cerebellar remyelination, which functionally improved cognitive and motor deficits of irradiated animals. Despite these exciting findings, the molecular pathways driving recovery of these pathological states require further investigation. Nonetheless, manipulating levels of OPC genes, including Olig2, Sox2, or TAPP1 have been shown to influence OPC recruitment and/or myelination thereby inferring the importance of external signaling pathways on this process, such as those induced by exercise (Chen et al., 2015; Wegener et al., 2015; Zhao et al., 2015).

Recently, we characterized mice inactivated for the *Snf2h* gene demonstrating that these animals have cerebellar hypoplasia, develop severe ataxia by postnatal day 20 (P20), and die between P25–P45 (Alvarez-Saavedra et al., 2014). At the cellular level, these mice generate significantly fewer granule and Purkinje cells (PC) within the cerebellum, accompanied by poor PC dendritic arborization. Molecularly, alterations in chromatin folding underlie the progressive death of surviving neurons. In this study, we assessed whether our model was receptive to exercise therapy and could be used to identify molecules and/or novel pathways that delayed the progression of this neurodegenerative phenotype. Here, we present evidence to suggest that the long-term survival of these mice is attained through voluntary exercise. Exercise induced the myelination of cerebellar neurons, amelioration of motor deficits and a significant extension of lifespan that was dependent on continued exercise or adenoviral-mediated VGF overexpression.

RESULTS

Voluntary Running Extends the Lifespan of *Snf2h* cKO Mice

To investigate the mechanisms linking exercise to neural protection, we made use of mice ablated for the chromatin remodeler Snf2h in the brain that develop a progressive neurodegenerative and ataxic phenotype (Alvarez-Saavedra et al., 2014). Conditional *Snf2h*-null mice have an abnormal gait with reduced weight gain by postnatal day 10 (P10), that progresses to classical signs of cerebellar ataxia by P20. Mice perform poorly in motor function tests at this age, continue to physically degenerate, show progressive Purkinje cell (PC) loss, and die between P25–P45 (Alvarez-Saavedra et al., 2014). Morphologically, the cerebellum of *Snf2h* cKO mice is one-third the size of control littermates due to a severe reduction in granule neuron progenitor expansion, coupled with the progressive death of PCs (Alvarez-Saavedra et al., 2014). Given the progressive nature of the phenotype and the collective finding that exercise can improve neurodegenerative disorders, we reasoned that the *Snf2h* cKO mice would be a good model to further examine the underlying mechanisms involved. To assess whether our model was receptive to exercise therapy, we provided them with unlimited access to a running wheel shortly after weaning (~P21–P23). Strikingly, voluntary running prolonged the survival of *Snf2h* cKO animals beyond 1 year of age (Figure 1A). Running was critical for long-term survival as a cohort of mice that received the running wheel at P21–P25 but had it removed at P100 showed a progressive decline and death between P150–P200 (Figure 1A). Along with survival, running increased weight gain in *Snf2h* cKO mice at a rate that was similar to wild-type littermate controls (Figure 1B). *Snf2h* cKO mice showed daily improvement in the distance traveled but overall averaged one-half the total traveled distance of control littermates (Figure 1C). Previously, we demonstrated that the *Snf2h* cKO mice have motor deficits, as they fell much quicker from either a small elevated platform or when placed on a rotarod, a rotating rod that increases in speed with time (Alvarez-Saavedra et al., 2014). As such, we repeated these assays with *Snf2h* cKO runner mice. Running improved performance in the rotarod assay (Figure 1D) and open field tests (Figures 1E–1G). Moreover, *Snf2h* cKO mice tested in the elevated platform and rotarod assays 50 days post-wheel removal displayed diminished performance compared to mice that continued to run (Figures 1H and 1I; Movies S1, S2, S3, S4, S5, S6, S7, and S8).

Voluntary Running Triggers Oligodendrogenesis, Myelination, and PC Dendritic Arborization of the Ataxic Cerebellum

Because physical exercise can trigger both neurogenesis and oligodendrogenesis in the murine forebrain (Krityakiarana et al., 2010; van Praag et al., 1999a), we next determined which process was active in hindbrain areas. Bromodeoxyuridine (BrdU) was administered via the drinking water (2 g/L) to label dividing cells between P21–P35 in wild-type controls (hereon referred to as WT) and *Snf2h* cKO mice (cKO hereon) provided with running wheels at P21. Whole brain sagittal sections through the deep cerebellar nuclei (DCN) of the cerebellum and the inferior olivary nucleus within the brain stem (also known as inferior olive), a major site of input into the cerebellum, were then analyzed either 55 or 145 days post-BrdU administration (P90 or 180, respectively) for $BrdU^+$ cells co-stained with the oligodendrocyte precursor (OP) or oligodendrocyte (OL) markers NG2 and Olig2, respectively. As expected, we observed prominent BrdU-labeling within the hippocampus in WT-Runner and cKO-Runner mice relative to sedentary controls (Figure S1). We did not detect any BrdU-labeled PCs in the cerebellum of any genotype (data not shown). However, cKO-Runner mice showed increased $BrdU^+/NG2^+$ cell numbers within the

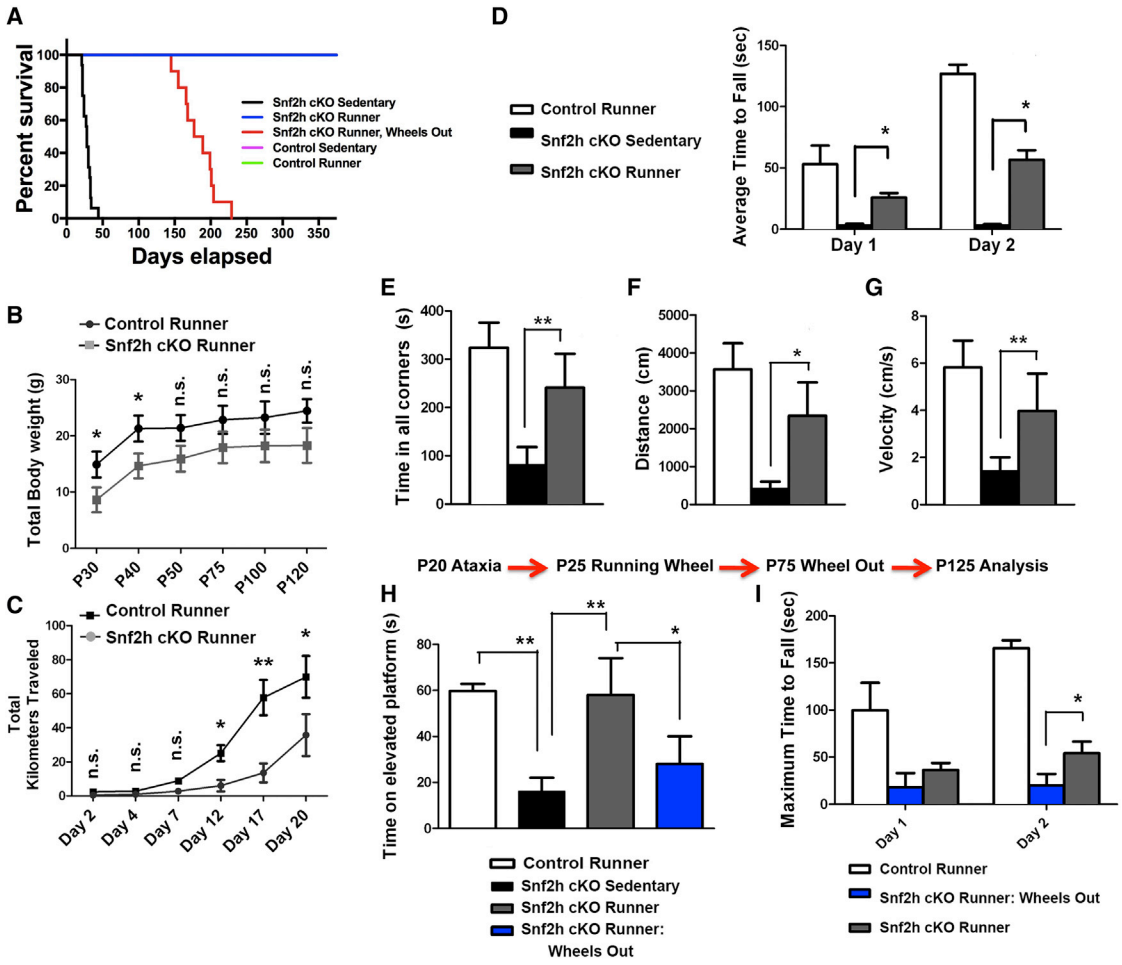

Figure 1. Voluntary Running Prolongs the Lifespan and Ameliorates the Motor Dysfunction of Snf2h-Null Ataxic Mice

(A) Kaplan-Meier curve for *Snf2h* cKO (cKO hereon) mice in sedentary (cKO-Sedentary; black) or running conditions (cKO-Runner) with wheels introduced at P21 and never removed (blue); or wheels removed at P100 (cKO-Runner, wheels out; red). Control sedentary and Control Runner mice were also included, but they're masked by the blue line. Analysis was terminated at 1 year of age (P365). n = 6–10 mice per condition.

(B) Total body weight of cKO-Runner or Control-Runner littermates with wheels introduced at P25. n = 8, males only. Error bars represent ± SEM. *p < 0.05, n.s., non-significant, n = 6–8 mice per condition.

(C) Total kilometers traveled for 20 days after wheels were introduced at P25. n = 8, males only. *p < 0.05, **p < 0.01, n.s., non-significant.

(D) Rotarod analysis for CT-Runner, cKO-Sedentary, and cKO-Runner mice for 2 consecutive days 15 days post-running (wheels in at P25). Note that CT-Sedentary mice behave identical to CT-Runner mice. *p < 0.05, n = 6–8 mice per condition.

(E–G) Open field assay for CT-Runner, cKO-Sedentary, and cKO-Runner mice 15 days post-running (wheels in at P25). Time in all corners (E), total distance traveled (F), and velocity (G) was averaged from 6–8 mice per genotype. *p < 0.05, **p < 0.01.

(H and I) Elevated platform (H) and rotarod assays (I) at P125 from WT-Sedentary, cKO-Sedentary, cKO-Runner, and cKO-Runner-wheels out mice (wheels in at P21–P25, wheels out at P75). *p < 0.05, **p < 0.01, n = 6–8 mice per condition.

See also Movies S1, S2, S3, S4, S5, S6, S7, and S8.

cerebellum and the brain stem (Figures 2A–2C, S2, and S3), suggesting that oligodendrogenesis may partially underlie the long-term recovery of ataxic exercising mice. Indeed, BrdU-retaining cells that co-expressed the differentiated OL marker Olig2 were significantly upregulated in cKO-Runners at P90 and P180 relative to all controls in both the cerebellum and inferior olive (Figure 2D). We additionally attempted to block oligodendrogenesis by administering 10 mg/kg trichostatin A (TSA) at P30, as has been recently described (Gibson et al., 2014), and co-administered EdU the following day for 3 consecutive days at 100 mg/kg. Cerebella were analyzed at P40 with double labeling for EdU and NG2, but we did not observe a significant decrease on the number of $NG2^+/EdU^+$ cells in the cerebella of Snf2h cKO-Runner mice with TSA or vehicle treatment (Figure S4). Because neurodegenerative pathologies are also associated with increased inflammation (Fernandes et al., 2014; Skaper, 2007), we assessed the total number of $Iba1^+$ microglia or $GFAP^+$ astrocytes within the cerebellum and inferior olive from all genotypes. This experiment revealed no changes in the total number of either Iba^+ or $GFAP^+$ cells (Figures 2E and 2F).

To assess whether the increased number of $Ng2^+$ and $Olig2^+$ OPs and OLs resulted in increased myelination, toluidine

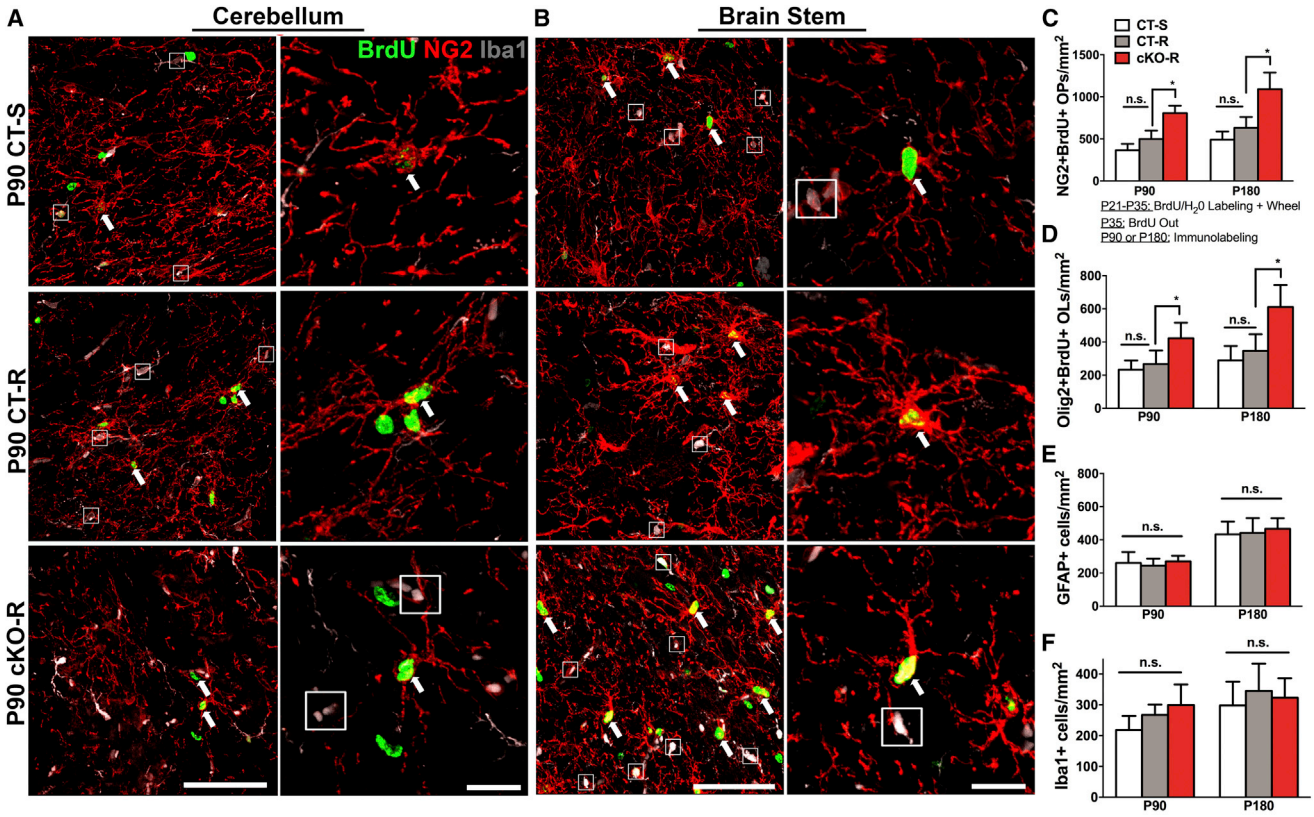

Figure 2. Voluntary Running Triggers the Expansion of Oligodendrocyte Precursors in the Ataxic Hindbrain

(A and B) Triple immunolabeling with BrdU (green), NG2 (red) and Iba1 (gray) through the (A) deep cerebellar nuclei of the cerebellum and (B) the inferior olivary nuclei within brain stem of WT-Sedentary, WT-Runner, and cKO-Runner mice when wheels were introduced at P21. BrdU was administered in the drinking water from P21–P35, and sagittal brain sections were analyzed at P90 (55 days post-BrdU labeling). Boxes highlight $BrdU^{-}$, $Iba1^{+}$ microglial cells, while arrows denote $BrdU^{+}$, $Ng2^{+}$ oligodendrocyte precursors (OPs). Note a robust increase in OPs within the cerebellum and brain stem of cKO-Runner mice. n = 4 mice per condition. Scale bars, 50 μm. See also Figure S3 for WT-Sedentary and cKO-Sedentary images at P40.

(C–F) Cell counts with the indicated markers from 1 mm^2 × 100 μm^3 confocal z stacks through the cerebellum and brain stem (pooled data) of WT-Sedentary, WT-Runner, and cKO-Runner mice treated with BrdU in the drinking water between P21–P35 (wheels in at P21) and analyzed 55 days post-BrdU removal (P90), or 145 days post-BrdU removal (P180). Error bars represent ± SEM. *$p < 0.05$, **$p < 0.01$, n.s. = not significant, n = 4 mice per condition.

See also Figures S1, S2, S3, and S4.

blue-stained and ultrathin transmission electron microscopy (TEM) images from the molecular layer and the white matter of the cerebellum were obtained from WT and cKO mice 125 days post-running (wheels introduced at P25) and from P25 WT and cKO sedentary mice as controls. Strikingly, we observed myelin rings surrounding most PCs in cKO-Runner mice that were not present in WT-Sedentary, WT-Runner, or cKO-Sedentary mice (Figures 3A, 3B, and S5A–S5C). As control, the white matter of the cerebellar lobes from all genotypes showed comparable myelination (Figure 3A, rightmost panels), as well as the sciatic nerves (Figure S5D). Myelination is not typically present within the molecular layer of the cerebellum and due to the disorganization of the mutant cerebellum, we were unable to determine if the myelination was present on axons of PCs projecting from a different plane, or derived from the parallel and climbing fibers of granule or inferior olivary neurons, respectively. Regardless, we speculated that increased myelination protects and strengthens the function of the existing neurons in the cerebellum of mutant mice. Because increased myelination confers improved neuronal function and because running activity was shown to improve PC dendritic arborization (Fernandes et al., 2014), we next examined the thickness of the molecular layer. Indeed, we observed a significant increase in the thickness of the molecular layer in both WT-Runner and cKO-Runner mice versus WT-Sedentary and cKO-Sedentary animals (Figures 4A–4D). These results are further supported as increased PC dendritic growth has been previously attributed to running activity in wild-type rodents (Pysh and Weiss, 1979). To further attribute this to a neuronal effect, we co-labeled WT and cKO Sedentary or Running (15 days post running; wheels in at P25) mice with the serotonin transporter (Slc4a6) and Calbindin, a marker of PCs. We observed increased Slc4a6 puncta within the PC soma of cKO-R mice relative to all control genotypes, suggesting that running enhanced the activity and survival of existing mutant PCs (Figure 4E). As an additional control, we performed histology on the transverse abdominal (TA) muscle of control and Snf2h

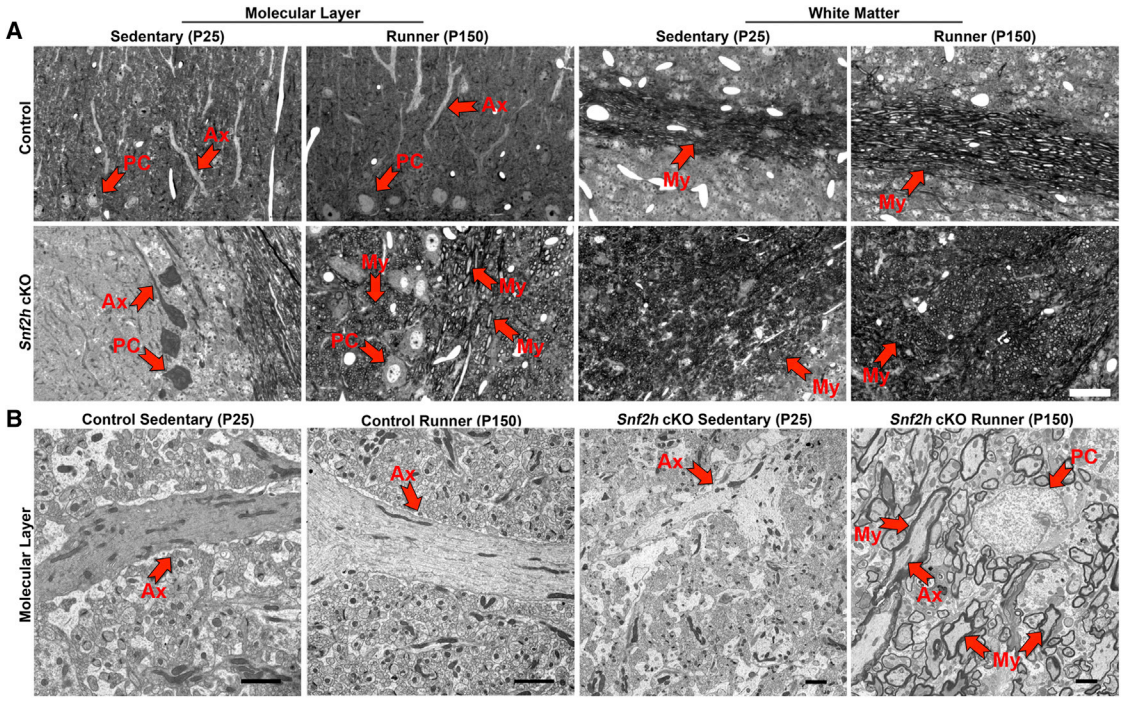

Figure 3. Voluntary Running Triggers the De Novo Myelination of the Ataxic Cerebellum

(A) Toluidine blue staining through the cerebellar vermis (molecular layer) and the deep cerebellar nuclei (white matter) of WT-Sedentary and cKO-Sedentary mice at P25 and WT-Runner and cKO-Runner mice at P150 (wheels in at P25). Note the massive appearance of myelin rings through the cKO-Runner cerebellum. PC, Purkinje cell; Ax, axon; My, myelin; n = 4 mice per genotype. Scale bars, 100 μm.

(B) Transmission electron microscopy (TEM) analysis within the molecular layer of WT and cKO-Sedentary mice at P25 and WT and cKO-Runner mice at P150 (wheels in at P25). Note the robust de novo myelination through neuronal processes in cKO-R cerebella. n = 4 mice per genotype. Scale bars, 2 μm.

See also Figures S5 and S6.

cKO sedentary and runner mice revealing no major structural differences among genotypes and conditions (Figure S6).

Comparative RNA Sequencing Analysis Identified Increased Levels of the VGF Neuropeptide

Concomitant to our cellular studies, we performed RNA-sequencing (RNA-seq) experiments to identify potential molecular correlates contributing to the exercise-induced rescue of cKO mice. While we recognize that some gene expression changes may arise from differences in certain cell types in the mutant cerebellum (i.e., reduced granule neurons), it provides a useful starting point to initiate molecular studies. We performed a four-way comparative analysis between samples sequenced from WT-Sedentary, WT-Runner, cKO-Sedentary, and cKO-Runner cerebella, identifying 2,290 upregulated and 1,321 downregulated genes in the cKO-R versus WT-R analysis (Figure 5; see Data S1 for complete gene lists). Gene Ontology (GO) analyses were consistent with our findings, namely that genes involved in neurotransmitter release and activity-dependent synaptic transmission (e.g., dopamine transporter [Slc6a3], noradrenaline transporter [Slc6a2], serotonin transporter [Slc6a4], choline transporter [Slc5a7], and vesicular monoamine transporter [Slc18a2], among others) were increased (Figure 6A). In addition, we observed an increase in growth factors (e.g., Dlk1 and Tdgf1) and the exercise-induced neuropeptide precursor protein VGF (Figure 6B) (Hunsberger et al., 2007). We validated VGF as well as several other neuropeptide precursor genes (e.g., chromogranin-B [ChgB], vasointestinal peptide [VIP], gastrin-releasing peptide [GRP], neuropeptide Y [NPY], and somatostatin [Sst], as well as brain-derived growth factor [BDNF], among others) to be significantly upregulated in cKO-Runner versus cKO-Sedentary cerebella and brain stems with TaqMan-based qPCR (Figure 6B). Lastly, we found that the VGF precursor protein is robustly and significantly upregulated in cerebella of Snf2h cKO-Runner mice relative to Snf2h cKO-Sedentary, Control-Sedentary, and Control-Runner mice after 15 days of running (wheels in at P25, analysis at P40; Figure 6C).

VGF Promotes the Proliferation and Differentiation of OP Cultures

The upregulation of the VGF gene was of particular interest because it was reported to be highly expressed in OPs (Dugas et al., 2006). Furthermore, its upregulation upon exercise activates the anti-depressant response in mammals and maintains BDNF expression in a VGF-BDNF-positive feedback loop (Alder et al., 2003; Bozdagi et al., 2008; Hunsberger et al., 2007). Moreover, reduced VGF peptide levels are considered biomarkers for both amyotrophic lateral sclerosis (ALS) and Alzheimer's disease, pathologies that have a demyelination component (Pasinetti et al., 2006; Selle et al., 2005). Hence, we next asked whether VGF

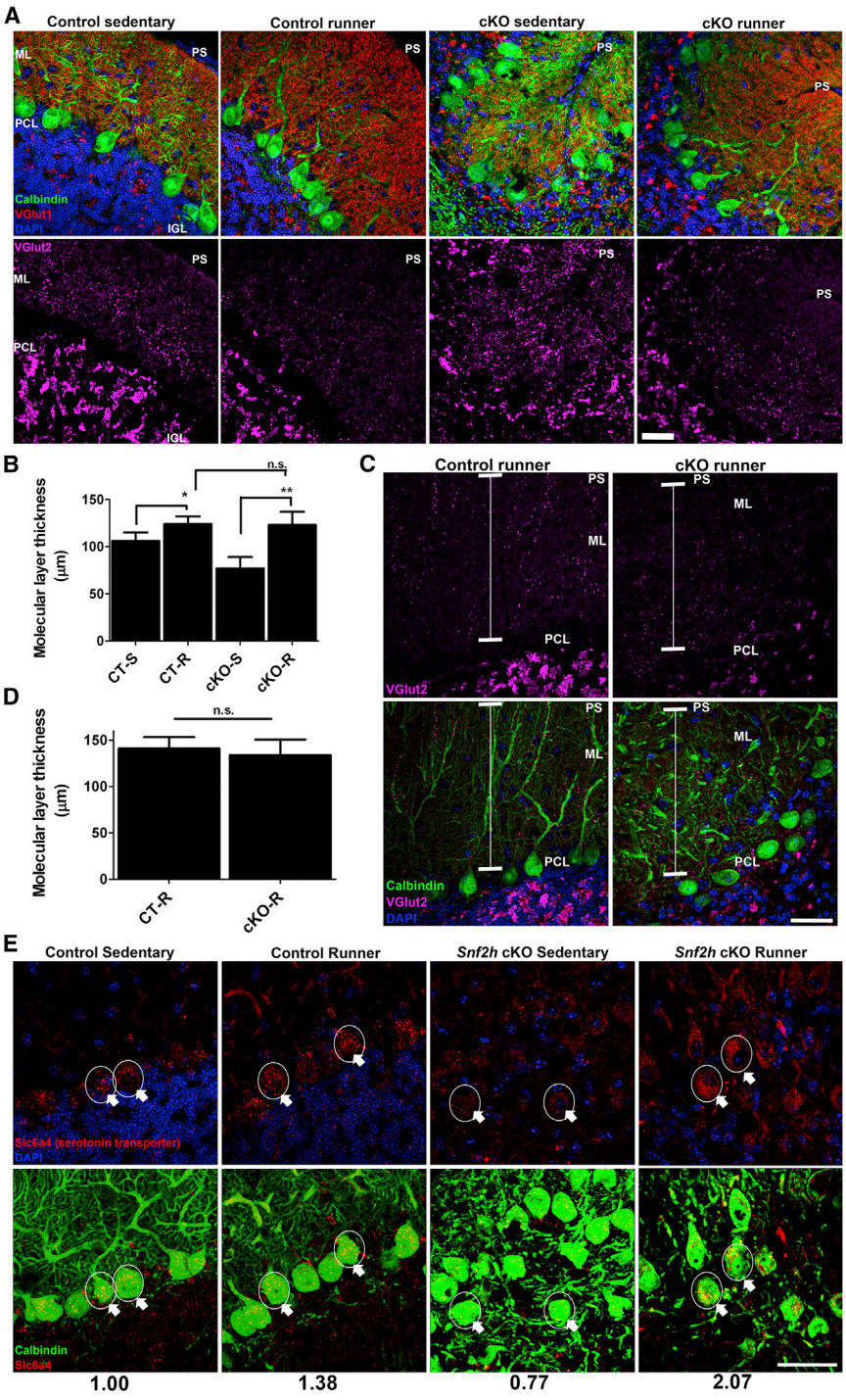

Figure 4. Voluntary Running Enhances PC Dendritic Arborization in WT and Ataxic Mice

(A and C) Triple immunolabeling through the molecular layer of WT-Sedentary, cKO-Sedentary, WT-Runner, and cKO-Runner at P40 (A) or at P300 (C) when wheels were introduced at P25 with the synaptic markers VGlut1 (red), VGlut2 (magenta), and Calbindin (green). DAPI (blue) stains all nuclei. Note the increased arborization of PCs in cKO-R cerebella at both time points. PS, pial surface; ML, molecular layer; PCL, Purkinje cell layer; IGL, internal granule layer; n = 4 mice per genotype. Scale bars, 20 μm.

(B and D) Quantitation of the molecular layer thickness of WT-Sedentary, cKO-Sedentary, WT-Runner, and cKO-Runner mice at P40 (B); or for WT-Runner and cKO-Runner mice at P300 (D) when wheels were introduced at P25. Error bars represent ± SEM. *$p < 0.05$, **$p < 0.01$, n.s. = not significant, n = 4 per condition.

(E) Co-immunolabeling with Slc6a4 (serotonin transporter; red) and Calbindin (green) through the cerebellar vermis of wild-type and *Snf2h* cKO mice in sedentary and running conditions at P41 (wheels introduced at P21). DAPI (blue, top panels) stains all nuclei. Note a robust increase in Slc6a4 levels within PC nuclei (arrows and circles) in cKO-Runner cerebella. n = 4 mice per genotype. Scale bars, 50 μm. Numbers represent average pixel intensity measurements (red channel, Slc6a4) from at least 40 PCs from four mice per genotype. Values were normalized to control sedentary PCs.

peptides could stimulate the growth and/or differentiation of homogenous preparations of primary cortical mouse OPs (O'Meara et al., 2011). VGF is cleaved to produce numerous C-terminal bioactive peptides including TLQP-62, TLQP-21, and AQEE-30, among others (Lewis et al., 2015). As such, we treated OP cultures with previously characterized peptides that trigger BDNF production TLQP-21 (3 μM), AQEE-30 (3 μM), BDNF (50 ng/μL), or DMSO along with the proliferation marker BrdU and analyzed them 48 hr later by scoring the number of $NG2^+/BrdU^+$ cells. In parallel, we also counted the total number of $NG2^+$ cells to assess endogenous proliferation. Interestingly, we observed a significant increase in the total number of $NG2^+$ cells and in the total number of proliferating $Ng2^+/BrdU^+$ OPs when treated with the TLQP-21 VGF peptide. In contrast, no significant differences were observed in any of the other treatments (Figure 7A). We next assessed differentiation of the cultures with the mature OL markers myelin-associated glycoprotein (MAG) and myelin basic protein (MBP), where we observed that TLQP-21 also increased the average oligodendrocyte dendritic length suggesting that this VGF peptide can promote both OP proliferation and their subsequent differentiation into OLs (Figures 7B and 7C). Indeed, VGF protein levels are robust early in the OP differentiation cascade (Figure S7). Taken together, these results raised the exciting possibility that VGF is impacting the OL lineage and contributes to the long-term survival of running cKO mice.

GENE ID	NAME	WT-S	WT-R	log2
NM_001080118	Med1	0.281	5.689	4.341
NM_009784	Cacna2d1	0.771	11.346	3.879
NM_001033324	Zbtb16	0.594	5.423	3.192
NM_013697	Ttr	59.938	396.161	2.725
NM_134110	Kcne2	0.595	3.695	2.634
NM_025312	Sostdc1	0.733	3.711	2.340
NM_013823	Kl	1.437	6.796	2.241
NR_040291	4930706D22Rik	1.606	6.811	2.084
NM_013613	Nr4a2	1.439	5.172	1.846
NM_001039386	Nelf	0.000	12.230	1.797
NM_011297	Rps24	0.000	9.556	1.797
NM_145994	Abi1	0.000	14.823	1.797
NM_015744	Enpp2	107.495	273.179	1.346
NM_015743	Nr4a3	2.201	5.562	1.338
NM_212473	Fam53b	3.944	9.921	1.331
NM_010220	Fkbp5	3.530	8.745	1.309
NM_027560	Arrdc2	2.165	5.278	1.286
NM_010444	Nr4a2	5.298	12.792	1.272
NM_172469	Clic6	3.335	7.515	1.172
NM_008587	Mertk	4.140	9.191	1.151
NM_007669	Cdkn1a	5.693	12.285	1.110
NM_001034115	Shank1	8.075	17.100	1.082
NM_001037709	Rusc2	7.419	15.148	1.030
NM_183023	Rims4	16.322	32.935	1.013
NM_029210	Sv2c	4.697	9.237	0.976
NM_030256	Bcl9l	3.287	6.431	0.968
NM_021366	Klf13	12.496	24.249	0.957
NM_001081212	Irs2	6.133	11.828	0.947
NM_030728	9930013L23Rik	3.611	6.892	0.932
NM_022312	Tnr	5.120	9.761	0.931

GENE ID	NAME	WT-R	cKO-R	log2
NM_010020	Slc6a3	0.065	6.764	6.704
NM_138942	Dbh	0.330	10.614	5.008
NM_009209	Slc6a2	0.112	3.428	4.931
NM_010484	Slc6a4	0.342	9.566	4.805
NM_027391	Iyd	0.177	4.716	4.733
NM_173391	Tph2	0.838	18.125	4.435
NM_173403	Slc10a4	0.238	5.104	4.422
NM_022025	Slc5a7	0.276	3.045	3.465
NM_010052	Dlk1	1.097	11.683	3.413
NM_172523	Slc18a2	1.128	11.451	3.343
NM_011909	Usp18	0.403	3.666	3.184
NM_009778	C3	0.332	2.869	3.112
NM_172898	Kirrel2	0.822	6.733	3.033
NM_011562	Tdgf1	1.101	8.871	3.010
NM_029530	330527O06Rik	0.873	6.649	2.929
NM_011854	Oasl2	0.908	6.346	2.805
NM_016672	Ddc	2.797	18.735	2.744
NM_009780	C4b	1.769	9.871	2.480
NM_029967	Adamtsl1	0.812	4.076	2.328
NM_011150	Lgals3bp	4.978	23.029	2.210
NM_009377	Th	2.646	12.239	2.210
NM_009846	Cd24a	4.510	20.795	2.205
NM_133775	Il33	10.216	45.099	2.142
NM_001037294	Alpk2	1.450	5.929	2.032
NR_003513	Neat1	14.847	55.603	1.905
NM_028673	Zdbf2	0.927	3.355	1.856
NM_010277	Gfap	68.051	238.270	1.808
NM_008812	Padi2	8.004	27.974	1.805
NM_001001892	H2-K1	6.667	22.392	1.748
NM_001039385	Vgf	9.280	29.708	1.679

GENE ID	NAME	cKO-S	cKO-R	log2
NM_001081493	Cartpt	1.156	7.164	2.631
NM_001142924	Tcf7l2	1.651	9.247	2.486
NM_145703	Kcnip2	1.538	6.159	2.002
NM_010020	Slc6a3	1.732	6.868	1.987
NM_011361	Sgk1	19.113	67.031	1.810
NM_001079902	Repin1	2.109	7.328	1.797
NM_001033132	Commd6	0.000	15.745	1.797
NM_001039386	Nelf	0.000	14.959	1.797
NM_001252453	Ptprs	0.000	30.904	1.797
NM_007841	Ddx6	0.000	4.459	1.797
NM_009080	Rpl26	0.000	11.146	1.797
NM_010840	Mthfr	1.572	5.187	1.722
NM_178761	Zfp672	1.587	5.120	1.690
NM_015743	Nr4a3	1.900	5.138	1.435
NM_016957	Hmgn2	2.615	7.026	1.426
NM_022029	Nrgn	17.897	45.920	1.359
NM_011627	Tpbg	1.618	4.058	1.327
NM_009753	Bicd1	2.097	4.917	1.230
NM_013642	Dusp1	10.967	25.042	1.191
NM_021302	Stk32c	5.557	12.318	1.148
NM_029530	330527O06Rik	3.089	6.751	1.128
NM_025633	Metap1d	5.416	11.286	1.059
NM_001159942	Plekhg1	2.680	5.575	1.057
NM_175427	Fam163b	5.176	10.724	1.051
NM_178745	Tmem229b	8.985	18.261	1.023
NM_212473	Fam53b	4.956	10.003	1.013
NM_011349	Sema3f	2.559	5.094	0.993
NM_011065	Per1	9.617	18.984	0.981
NM_007669	Cdkn1a	9.660	18.800	0.961
NM_010220	Fkbp5	6.853	13.158	0.941

GENE ID	NAME	WT-S	cKO-S	log2
NM_027391	Iyd	0.151	5.294	5.128
NM_144944	Prokr2	0.211	4.887	4.535
NM_172898	Kirrel2	0.781	8.946	3.517
NM_013697	Ttr	61.528	498.802	3.019
NM_009846	Cd24a	3.672	28.409	2.952
NM_013823	Kl	1.476	10.636	2.850
NM_001037294	Alpk2	1.123	7.551	2.749
NM_010052	Dlk1	1.631	8.582	2.396
NM_009780	C4b	1.906	9.303	2.287
NM_133775	Il33	10.195	45.830	2.168
NM_009109	Ryr1	1.389	5.981	2.106
NM_008812	Padi2	7.681	32.043	2.061
NM_029210	Sv2c	4.822	18.920	1.972
NR_003513	Neat1	18.084	63.756	1.818
NR_033520	Tmem181b-ps	100.830	25.811	-1.966
NM_001170800	Ipcef1	19.746	5.052	-1.967
NM_028052	Synpr	51.974	12.985	-2.001
NM_010551	Il16	38.720	9.652	-2.004
NR_028305	Tmem181c-ps	31.014	7.702	-2.010
NM_153458	Olfm3	79.954	19.696	-2.021
NM_019626	Cbln1	226.905	55.831	-2.023
NM_178110	Trim62	57.104	13.695	-2.060
NM_177292	Wscd2	45.375	10.779	-2.074
NM_009527	Wnt7a	20.869	4.691	-2.153
NM_008072	Gabrd	74.380	15.498	-2.263
NM_153420	Acpl2	16.768	3.426	-2.291
NM_019465	Crtam	32.190	5.934	-2.440
NM_007586	Calb2	262.911	47.349	-2.473
NM_001099641	Gabra6	330.818	58.756	-2.493
NM_007662	Cdh15	18.506	3.209	-2.528

(legend on next page)

Adenoviral-Encoded Full-Length VGF Delivery Increased Myelination and Prolonged the Lifespan of *Snf2h*-Null Ataxic Mice

To determine whether VGF was sufficient to rescue the lifespan of cKO mice, we generated adenoviral (Ad) vectors expressing full-length mouse VGF protein (Ross and Parks, 2009). Control and sedentary cKO mice received tail vein injections at ~P21 (1×10^{12} viral particles/kg) and their survival was recorded. Strikingly, cKO mice that received the Ad-VGF injections were alive and healthy at P300 (time of analysis) whereas uninjected cKO or Ad-control (no VGF cDNA)-injected cKO mice perished between P25 and P45 using both C57Bl/6 and FVB/N backcrossed cKO strains (Figure 7D). Using qPCR to compare transcript levels between cKO Ad-control and cKO Ad-VGF, we were able to detect significant VGF mRNA upregulation in the heart, hippocampus, cerebellum, and brain stem, with highest levels in the liver, the primary site of adenoviral transduction (Figure 7E). However, we only detected upregulation of the BDNF transcript in the brain (hippocampus, cerebellum, and brain stem) and not in any of the other tissues analyzed (Figure 7E). Importantly, TEM images demonstrated increased myelination in the molecular layer of the cerebellum and within the brain stem of cKO Ad-VGF-treated animals versus WT Ad-VGF- or cKO Ad-control-treated mice, suggesting that increasing cerebellar myelination was critical for the survival of the sedentary cKO mice (Figures 7F–7H). Notably, we did observe some additional, but non-significant myelination in Ad-VGF-injected WT animals, but it was minimal compared to the rescued Ad-VGF-treated sedentary cKO mice. Moreover, we observed a significant increase in the number of NG2-BrdU and Olig2-BrdU double-positive cells in the cerebella of Snf2h cKO mice treated with Ad-VGF relative to all other treatments (Figures 7I and 7J). This was also accompanied by increased levels of the VGF propeptide in the plasma of cKO mice treated with Ad-VGF and not with Ad-CT (Figure 7K).

DISCUSSION

Exercise induces the secretion of several hundred peptides from skeletal muscle (myokines) that are known to exert autocrine, paracrine, and endocrine effects on multiple tissues, including the brain. Many of these myokines promote metabolic homeostasis and, collectively provide protective effects against obesity, diabetes, cardiovascular, and neurodegenerative disease (Pedersen and Febbraio, 2012; Pedersen et al., 2009). Given the dependence of exercise on the long-term survival of *Snf2h* cKO mice, these systemic effects are key contributors to the recovery of these mice. In this regard, many studies have shown that exercise induces BDNF to promote neurogenesis, and exercise mimetics such as AICAR analogs and metformin similarly promote neurogenesis via BDNF (Dadwal et al., 2015; Kobilo et al., 2011; van Praag et al., 1999a, 1999b, 2005; Wang et al., 2012). However, within the cerebellum we did not observe enhanced neurogenesis but rather increased oligodendrogenesis suggesting that the primary mechanism was distinct. Moreover, the comparative RNA-seq data indicated an upregulation of VGF, a neuropeptide precursor that: (1) is similarly induced by exercise within the hippocampus (Hunsberger et al., 2007); (2) has widespread influences on energy metabolism, antidepressant effects, neurogenesis, and learning (Bartolomucci et al., 2006; Hahm et al., 1999; Hunsberger et al., 2007; Thakker-Varia et al., 2007, 2014); and (3) it is highly expressed in OPs (Dugas et al., 2006). Indeed, we demonstrated that VGF could induce oligodendrogenesis in vitro and that adenoviral delivery of the full-length VGF precursor could significantly rescue the survival of the *Snf2h* cKO mouse model and trigger de novo myelination of cerebellar neurons to ameliorate motor deficits and prolong their lifespan.

A key pending question is how does VGF impact the repair process in the *Snf2h* cKO mice? It is known that exercise induces VGF in the hippocampus and that this promotes the anti-depressant effects caused by running (Hunsberger et al., 2007; Thakker-Varia et al., 2007). It also functions in a positive feedback loop to maintain BDNF expression (Hunsberger et al., 2007). Studies on cultured hippocampal neurons have shown that VGF peptides stimulate multiple signaling cascades to enhance synaptic activity (Alder et al., 2003; Bozdagi et al., 2008). Thus, within the cerebellum of the *Snf2h* cKO mice, the VGF peptides may serve to maintain the survival of the existing neurons and concomitantly, increase their synaptic activity, which would bolster cerebellar-dependent motor function. Consistent with this hypothesis, we observed increased expression of genes involved in serotonin, norepinephrine and dopamine synthesis, and enhanced dendritic arborization of PCs. Whether this is a direct or indirect effect of increased VGF expression requires further validation. Other studies have shown that BDNF released from astrocytes can also promote oligodendrogenesis (Miyamoto et al., 2015). Surprisingly, we did not observe an effect of BDNF on our in vitro OP cultures, although we did observe increased BDNF levels in the brain following VGF adenoviral treatment of the mice. While we cannot explain our in vitro results, our in vivo data suggest that VGF may be able to stimulate astrocytes to release BDNF and promote oligodendrogenesis indirectly.

Neuronal damage and neuronal loss results in the recruitment of OPs and differentiation into OLs (Brousse et al., 2015; Piao et al., 2015). Similarly, other studies have indicated that neuronal activity stimulates myelination to strengthen active circuits (Gibson et al., 2014). Importantly, demyelinated axons are electrically active and can generate de novo synapses with recruited OPs to facilitate OL differentiation and repair (Gautier et al.,

Figure 5. Voluntary Running Stimulates Synaptic Transmission and Growth Factor-Related Pathways

RNA-seq reveals the top 30 differentially expressed genes (DE) between cerebella from all genotypes after 15 days of running (wheels in at P25). Note the upregulation of a high number of genes (in the WT-R versus cKO-R comparison, top right table) involved in neurotransmitter release and activity-dependent synaptic transmission (cyan; e.g., TH, tyrosine hydroxylase; Slc6a3, dopamine transporter; Slc6a2, noradrenaline transporter; Slc6a4, serotonin transporter; DBH, dopamine beta-hydroxylase; Slc5a7, choline transporter; Tph2, tryptophan hydroxylase; as well as upregulation of neuropeptides [yellow] and the nerve growth factor-inducible gene VGF [green]). $p < 0.05$, $n = 2$ paired-end libraries per genotype. See also Data S1 for DE analyses between all four genotypes (WT-Sedentary versus WT-Runner, cKO-Sedentary versus cKO-Runner, WT-Sedentary versus cKO-Sedentary, and WT-Runner versus cKO-Runner).

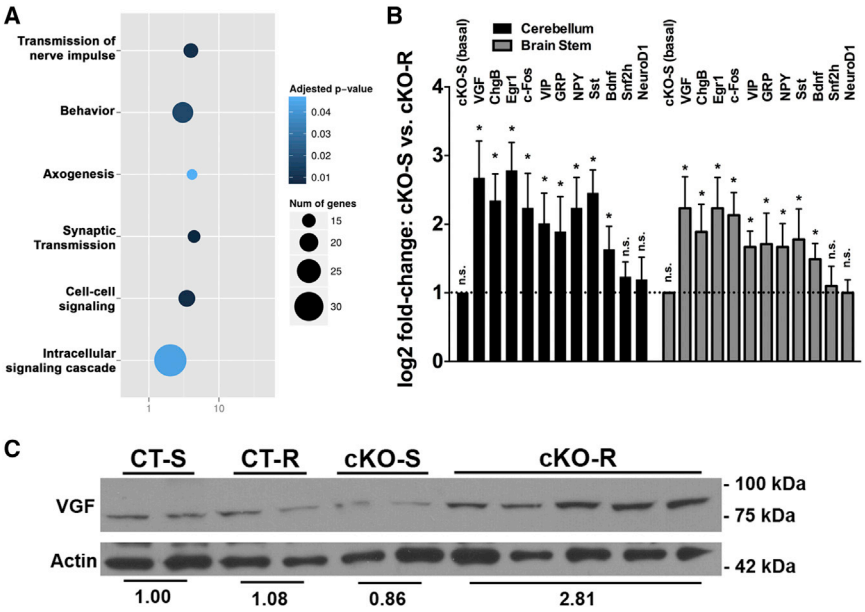

Figure 6. Voluntary Running Triggers Growth Factor Synthesis in the Ataxic Cerebellum and Brain Stem

(A) Gene Ontology (GO) biological processes enriched in upregulated gene sets from cKO-Runner versus WT-Runner cerebella. Selected genes were analyzed by DAVID for enriched GO terms and shown with Benjamini adjusted p values of <0.05.

(B) TaqMan probe-based qPCR validation for selected growth factors and immediate early genes between cKO-Runner versus cKO-Sedentary cerebella and brain stems. L32 was used as internal control. *p < 0.05, n.s. = not significant, n = 4 per condition.

(C) Western blotting with VGF antisera of cerebellar extracts from sedentary mice at P40 or from running mice at P40 after 15 days of running. Actin served as loading control. Pixel intensity measurements are provided below. n = 5 mice per genotype, per condition.

2015). Indeed, myelin is the most effective means of speeding conduction velocity by altering how electric potentials propagate. Most recently, cultured OPs were shown to preferentially myelinate electrically active axons, but OP-neuronal synapses were not required for activity-dependent myelination. One possible regulatory mechanism is through calcium signaling produced by vesicular release of glutamate, cellular effects that are also similarly mimicked by aerobic activity (Wake et al., 2015). Because both OPs and neurons express VGF, one possibility is that OPs and neurons utilize VGF peptides as a secreted molecular tool to express their relative health or activity to the other cell, in synapse-dependent and independent manners. In this regard, reduced VGF is a biomarker for several neurodegenerative diseases, including ALS and Alzheimer's disease, and is also downregulated in human bipolar postmortem brain tissue (Ferri et al., 2011; Pasinetti et al., 2006; Selle et al., 2005; Thakker-Varia et al., 2010). Moreover, the TLQP-21 peptide prevented apoptotic death of cerebellar granule neurons and exogenous induction of VGF in a mouse model of ALS attenuated excitotoxic injury, slowed disease progression, and prolonged survival (Severini et al., 2008; Shimazawa et al., 2010; Zhao et al., 2008). We demonstrated that VGF peptides were capable of promoting OP proliferation and differentiation into OLs using primary mouse OP cultures. While the mechanism(s) remains to be elucidated, future studies using cell-type-specific VGF cKO mice could shed light on whether VGF peptides function as secreted vehicles that mediate OL-neuron intercommunication to control activity-dependent synaptic remodeling and repair.

Inactivation of the *Snf2h* gene in the brain results in progressive cerebellar degeneration and death during early adulthood. Strikingly, voluntary running or intravenous full-length VGF delivery rescued the long-term survival of these animals (Figure 7L). Taken together, our results suggest that damaged cerebellar neurons can be substantially rescued by increased myelination, utilizing an endogenous mechanism of brain repair. It is now clear that OPs are the largest population of dividing cells in the adult brain, hence intrinsically implicated in activity-dependent myelination of the postnatal brain. Additionally, white matter structure can change with environmental experience and functional activity (Zatorre et al., 2012). In a normally functioning cerebellum, additional myelination is not as significant as in the pathological state, suggesting that exercise promotes a repair mechanism that counteracts a neurodegenerative process. How OP-neuron intercommunication changes during development in healthy and pathological states and in response to environmental stimuli are current areas of intense investigation. For the first time, our results provide strong evidence that VGF has the ability to stimulate OP proliferation, trigger myelination, revert neural damage, and prolong lifespan in our chosen disease model. These findings thereby illuminate a novel pathway to potentially treat other neuronal and/or oligodendroglia-associated pathologies of the CNS.

EXPERIMENTAL PROCEDURES

Mouse Breeding

Snf2h$^{fl/fl}$ mice (Alvarez-Saavedra et al., 2014) were backcrossed for six generations to a C57BL/6 or FVB/NCrl background and bred with a C57Bl/6 Nestin-Cre$^{-/+}$ heterozygous mice (Bérubé et al., 2005) that also carried a *Snf2h*-null allele (Stopka and Skoultchi, 2003), thereby generating *Snf2h* cKO mice by Nestin-Cre (*Snf2h*$^{-/fl}$::Nes-Cre$^{-/+}$ or *Snf2h* cKO) and control littermates that carried only one functional copy of *Snf2h* (*Snf2h*$^{-/fl}$ or *Snf2h*$^{+/fl}$::Nes-Cre$^{-/+}$) or both functional alleles (*Snf2h*$^{+/fl}$).

Behavioral Analysis

All behavioral tests were completed in the Behavior Core Facility at the University of Ottawa using standardized protocols. Animals were habituated to the testing room at least ~1 hr before testing. Behavioral assays were performed irrespective of sex. One-way ANOVA was used for at least 10–20 mice per genotype. The values are presented as the mean ± SEM.

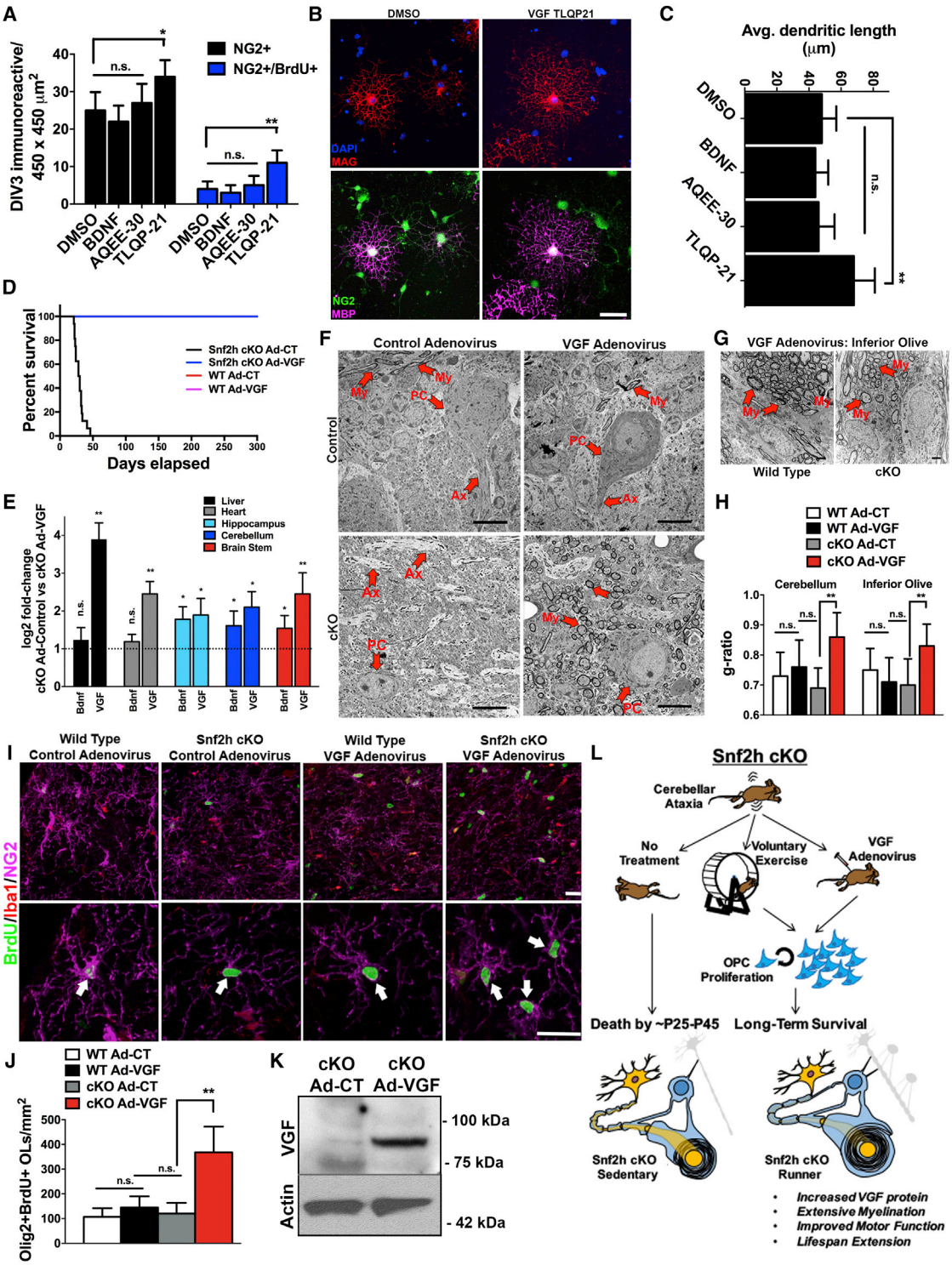

Figure 7. VGF TLQP-21 Stimulates OP Expansion and Differentiation In Vitro, While Full-Length VGF Overexpression Prolongs the Lifespan and Triggers De Novo Myelination of the Ataxic Cerebellum

Mouse OPs were isolated from the cortices of P0 WT neonates by expansion within mixed glial culture for 8 days, purified, and subsequently differentiated as an OP-enriched culture. At DIV1 post-purification, cells were treated with DMSO, BDNF (50 ng/μL), VGF AQEE-30, or VGF TLQP-21 at 3 μM and allowed to grow for an additional 48 hr.

(A) In a parallel experiment, cells were further supplemented with BrdU (20 nM) 6 hr after peptide or DMSO treatment and BrdU$^+$, NG2$^+$, or total NG2$^+$ cells counted in 450 × 450 μm^2 bins 42 hr post-BrdU treatment. *p < 0.05, **p < 0.01, n = 4 independent coverslips per condition.

(legend continued on next page)

BrdU-Birthdating

BrdU was diluted in nanopure water at a final concentration of 2 g/L and supplemented with 1% sucrose and protected from light. BrdU-containing water was changed with fresh stock every other day. Mice were given BrdU 2 days post-wheel introduction at P23 and allowed to drink freely for a maximum of 15 days (stopped at P40). Mice were then analyzed 50 days or 140 days post-BrdU removal (P90 or P180).

TSA and EdU Administration

Mice were single-housed and a running wheel was introduced between P21 and P25. TSA was administered intraperitoneally at 10 mg/kg at P30, and EdU was administered intraperitoneally the following day for 3 consecutive days at 100 mg/kg. Brains were analyzed at P40 and immunolabeled as described below. Cell counts were performed with the indicated markers from 1 mm^2 × 100 μm^3 confocal z stacks through the cerebellar lobes.

Immunofluorescent Histochemistry

Brain sections were obtained as 40–50 μm free-floating sections after cryopreservation. Sections were washed four times in PBS with 0.1% Triton X-100 (PBST), blocked (1 hr, room temperature [RT]) in 10% horse serum/PBST, and incubated (overnight, 4°C) in primary antibodies. Primary and secondary antibodies are listed in the Supplemental Information.

Reverse Transcription and Quantitative Real-Time PCR

Tissues were quickly dissected from mutant and control littermates and RNA was isolated using Trizol (Invitrogen) according to the manufacturer's instructions and further concentrated with RNeasy MinElute Cleanup Kits (QIAGEN). Glycogen (Ambion Life Technologies) was used as carrier. Total RNA (1 μg) was reverse-transcribed using SuperScriptIII (Invitrogen Life Technologies). cDNA was further diluted 1:10 and 1 μl was used per qPCR reaction. qPCRs were carried out using TaqMan probes (Applied Biosystems). Student's t test was used for statistical significance.

Western Blotting

Protein samples were resolved on SDS polyacrylamide gels under denaturing conditions or using Bis-Tris 4%–12% gradient gels (NuPage, Invitrogen) and blotted onto PVDF membranes (Immobilon-P; Millipore) by wet transfer for 1–2 hr at 90 V. Membranes were blocked (45 min, room temperature) with 5% skim milk in Tris-buffered saline containing 0.05% Triton X-100 (TBST), and incubated (4°C, overnight) with the following antibodies: rabbit anti-VGF (1:1,000; a kind gift from Dr. Stephen Salton) or mouse anti-β-Actin (1:30,000, Sigma). Western blots were quantitated using ImageJ software (rsbweb.nih.gov/ij/). At least three to five individual lanes from multiple litters were used for quantitation.

Cell Culture

Primary mouse oligodendrocyte precursor cells (OPCs) were harvested and propagated using an adaptation of the "shake-off" method originally described by McCarthy and de Vellis (1980). In brief, neonatal mouse cortices were dissociated and seeded onto poly-L-lysine (PLL)-coated flasks and grown as a mixed glial culture for 10 days. OPCs were then detached from the mixed glial cell monolayer via orbital shaking, and the purified OPC population was seeded onto poly-D-lysine, PLL, or laminin-coated coverslips and differentiated for up to 6 days. For immunolabeling, OPCs were fixed with 3% paraformaldehyde (PFA) for 15 min at room temperature (RT) and washed in PBS (0.1 M). Cells were then permeabilized with a 0.1% Triton X-100 solution for 10 min at RT and subsequently washed in PBS. A 10% goat serum blocking solution was then applied for 40 min, followed by an overnight incubation (4°C) with primary antibodies diluted in blocking buffer: myelin-associated glycoprotein (1:100, EMD Millipore), NG2 chondroitin sulfate proteoglycan (1:250, EMD Millipore), myelin basic protein (1:100, AbD Serotec), VGF (1:100; a kind gift of Dr. Stephen R. Salton, Mount Sinai Medical School, NY, USA), and chromagranin-B (1:100, Synaptic Systems #259103). For BrdU incorporation, purified OPCs were pulsed with 20 nM BrdU and subsequently fixed with 3% PFA, PBS washed, and permeabilized as described above. Prior to immunostaining, the cells were treated with 2 N HCl for 20 min under mild agitation. Neutralization was then achieved through addition of an equal volume of basic 0.1 M Tris-HCL for 20 min. Samples were processed for immunostaining as above, using an anti-BrdU antibody (1:200, Abcam #ab6326).

VGF TLQP-21 Peptide Treatments

Purified OPCs were differentiated in media containing either mouse VGF TLQP-21 (Bachem, #H-7272) or AQEE-30 (Bachem, #H-7276), BDNF

(B) At DIV3 post-purification, cells were triple immunolabeled with NG2 (green), a marker of OPs; MAG (red), a marker of differentiating OLs; and MBP (magenta), a marker of myelin-associated glycoprotein. DAPI (blue) stains all nuclei. Note the enlarged processes in OLs treated with VGF TLQP-21 versus DMSO controls. Scale bar, 10 μm.

(C) Quantitation of the average dendritic length 48 hr post-peptide treatment. **$p < 0.01$, n = 4 independent coverslips per condition.

(D) Early region 1 (E1)/E3-deleted adenoviral vectors driving an empty cassette (Ad-Control) or full-length mouse VGF (Ad-VGF) under the regulation of the human CMV promoter were delivered via tail-injection at ~P21 in cKO-Sedentary mice. Kaplan-Meier curves highlight the extended lifespan of cKO-Sedentary mice treated with Ad-VGF viral particles (blue line) relative to cKO-Sedentary mice treated with Ad-Empty control (black line). Experiments were terminated at P300 for tissue analysis.

(E) Taq-Man probe-based qPCR expression analysis for BDNF and VGF in selected tissues 30 days after viral delivery (~P51). L32 was used as internal control. *$p < 0.05$, **$p < 0.01$, n.s. = not significant, n = 4 per genotype.

(F and G) TEM analysis through the molecular layer of the cerebellum (F) or the inferior olive (G) of WT-Sedentary and cKO-Sedentary mice at P60 treated with empty Ad-CT or Ad-VGF vectors at ~P21. Note the robust myelination in the cerebellum of Ad-VGF-treated cKO mice. PC, Purkinje cell; My, myelin; Ax, axon; n = 4 mice per genotype from two independent experiments. Scale bars, 10 μm.

(H) G-ratios of axons within the molecular layer of the cerebellum and the inferior olive of WT-Sedentary and cKO-Sedentary mice at P60 treated with empty Ad-CT or Ad-VGF vectors at ~P21. **$p < 0.01$, n.s., non-significant; ~50 axons were scored from four independent mice per genotype from two independent experiments.

(I) BrdU (green), Iba1 (red), and NG2 (magenta) triple-immunolabeling through the deep cerebellar nuclei of the cerebellum of WT-Sedentary and cKO-Sedentary mice at P50 treated with empty Ad-CT or Ad-VGF vectors at ~P21. n = 4 mice per genotype. Scale bars, 20 μm.

(J) Cell counts at P50 with the indicated markers from 1 mm^2 × 100 μm^3 confocal z stacks through the deep cerebellar nuclei of WT-Sedentary and cKO-Sedentary mice treated with empty Ad-CT or Ad-VGF viral vectors at ~P21. Error bars represent ± SEM. **$p < 0.01$, n.s., non-significant, n = 4 mice per condition.

(K) Western blotting of isolated plasma with VGF antisera from cKO mice at P50 treated with empty Ad-CT or Ad-VGF vectors at ~P21. Actin served as loading control.

(L) Proposed model of running-induced de novo myelination of the dying brain. Sedentary *Snf2h* cKO (ataxic) mice perish between P25–P45. When a wheel is introduced for voluntary running, *Snf2h* cKO show oligodendrocyte precursor cell (OPC) expansion and extensive de novo myelination of otherwise dying Purkinje neurons. This OPC expansion and de novo myelination can also be mimicked with adenoviral-mediated full-length VGF precursor protein delivery in the absence of exercise. Upon running or VGF overexpression, ataxic *Snf2h* cKO mice show increased VGF protein in the plasma and brain, extensive myelination of damaged cerebella, improved motor function, and a significant extension of their lifespan. VGF, nerve growth factor-inducible; P, postnatal; cyan cell, OPC; yellow cell, neuron; light blue cell, mature oligodendrocyte.

See also Figure S7.

(Sigma-Aldrich, #B3795), or DMSO at 3 μM. Cells were then processed for immunofluorescence as described above.

RNA-Sequencing and Bioinformatics

Tissues were quickly dissected from mutant and control littermates and RNA was isolated using Trizol (Invitrogen) according to the manufacturer's instructions and further concentrated with RNeasy MinElute Cleanup Kits (QIAGEN). Glycogen (Ambion Life Technologies) was used as carrier. We pooled three independent cerebella as one sample per genotype and sequenced two independent pools per genotype using Illumina HiSeq 2000 paired-end technology at McGill University and Genome Quebec Innovation Center. Bioinformatics pipeline is described in the Supplemental Information.

Adenoviral Construction and Delivery

A plasmid containing the murine VGF cDNA (a kind gift of Stephen Salton, Mount Sinai School of Medicine), was digested with HindIII, the ends repaired with T4 DNA polymerase, digested with NotI, and the fragment cloned into EcoRV/NotI digested pRP2645 (Poulin et al., 2010), generating pRP3137. As such, in pRP3137 full-length murine VGF was placed under regulation of the human cytomegalovirus immediate-early enhancer/promoter and bovine growth hormone polyadenylation sequence. The expression cassette contained in pRP3137 was cloned into an adenovirus type 5 genomic plasmid, pRP2014 (Poulin et al., 2010), using RecA-mediated bacterial recombination, generating pRP3140 (Chartier et al., 1996; Ross and Parks, 2009). pRP3140 was transfected into HEK293 cells and then propagated and purified using standard techniques (Ross and Parks, 2009). Thus, AdRP3140 is an early region 1 (E1)/E3-deleted Ad vector containing the mVGF under regulation by the human CMV promoter and BGHpA. An empty adenoviral construct was used as control. Mice were given a single dose via tail injection of 1×10^{12} viral particles per kilogram (VP/kg) diluted in a 100-μL final volume. At least 10–15 mice were injected per genotype per condition.

Image Acquisition and Processing

Tissue sections were examined and images captured using a Zeiss 510 laser scanning confocal microscope with UV (405 nm), argon (488 nm), helium/neon (546 nm), and helium/neon (633 nm) lasers. All images were acquired as 30 μm z stacks (in 1- to 2-μm intervals) and analyzed as projections using the LSM 510 Image Browser software (Zeiss). Images were exported to Adobe Photoshop CS5 (Adobe Systems) and further processed for contrast when necessary.

Toluidine Blue Staining

Semi-thin sections of 0.5 μm were stained with 1% toluidine blue and 2% Borate in distilled water. Histological samples were scanned with a MIRAX MIDI automated scanning light microscope (Zeiss) and images processed with Zeiss MIRAX Viewer software (Zeiss).

Transmission Electron Microscopy

Cerebella vermis, deep cerebellar nuclei, brain stem, and inferior olive brain regions were collected under a stereomicroscope, cut into sections of 1- to 2-mm thickness and fixed for at least 4 hr to overnight in Karnovsky's fixative (4% paraformaldehyde, 2% glutaraldehyde, and 0.1 M cacodylate in PBS [pH 7.4]) at 4°C. Grids were stained with 2% aqueous uranyl acetate and with Reynold's lead citrate. Sections were observed under a transmission electron microscope (TEM) (Hitachi 7100). All ultrastructural analysis were based on at least three mice per genotype of the same age for each group examined.

Statistics

Group statistical analysis was performed via a two-tailed Student's t test or one-way ANOVA where indicated; $p < 0.05$ was accepted as statistically significant. At least three mice from each genotype were used for evaluation. The values are presented as the mean ± SEM. For BrdU or EdU cell counting in the cerebellar lobes and brain stem, three 1-mm^2 regions in 100 μm^3 cubic z stacks were counted per animal, n = 4 mice per genotype.

ACCESSION NUMBERS

The accession number for the RNA sequencing data reported in this paper is GEO: GSE86235.

SUPPLEMENTAL INFORMATION

Supplemental Information includes Supplemental Experimental Procedures, seven figures, eight movies, and one data file and can be found with this article online at http://dx.doi.org/10.1016/j.celrep.2016.09.030.

AUTHOR CONTRIBUTIONS

M.A.-S. designed, executed, analyzed, and interpreted all experiments. D.J.P. supervised the project. Y.D.R., R.W.O., and R.K. performed TEM and OP cell culture experiments. L.R., D.E.B., D.Y., and I.I. provided bioinformatics support. K.Y. and L.E.H. provided technical support. R.J.P. cloned and packaged adenoviral vectors. M.A.-S. and D.J.P. wrote the paper.

ACKNOWLEDGMENTS

We thank Dr. Diane Lagace and Mirela Hasu at the University of Ottawa's Behavioral Core for assistance with behavioral experiments and expert discussions. We are grateful to Dr. Michael Schlossmacher (OHRI) for critically reading the manuscript. We thank Theresa Falls and Dr. John Bell for assistance with tail-vein injections (OHRI). We are also grateful to Dr. Stephen R. Salton for mouse VGF antibodies and full-length mouse VGF vectors (Mount Sinai School of Medicine) and John Alberta for Olig2 antibodies (Harvard Medical School). This work was funded by operating grants from the Canadian Health Research Institutes to D.J.P. (MOP133586 and MOP142398). M.A.-S. thanks D.J.P. for funding and the Pew Charitable Trusts for a Pew Latin American Postdoctoral Fellowship.

Received: December 21, 2015
Revised: July 20, 2016
Accepted: September 9, 2016
Published: October 11, 2016

REFERENCES

Abbott, R.D., White, L.R., Ross, G.W., Masaki, K.H., Curb, J.D., and Petrovitch, H. (2004). Walking and dementia in physically capable elderly men. JAMA *292*, 1447–1453.

Alder, J., Thakker-Varia, S., Bangasser, D.A., Kuroiwa, M., Plummer, M.R., Shors, T.J., and Black, I.B. (2003). Brain-derived neurotrophic factor-induced gene expression reveals novel actions of VGF in hippocampal synaptic plasticity. J. Neurosci. *23*, 10800–10808.

Alvarez-Saavedra, M., De Repentigny, Y., Lagali, P.S., Raghu Ram, E.V., Yan, K., Hashem, E., Ivanochko, D., Huh, M.S., Yang, D., Mears, A.J., et al. (2014). Snf2h-mediated chromatin organization and histone H1 dynamics govern cerebellar morphogenesis and neural maturation. Nat. Commun. *5*, 4181.

Barnes, J.N. (2015). Exercise, cognitive function, and aging. Adv. Physiol. Educ. *39*, 55–62.

Bartolomucci, A., La Corte, G., Possenti, R., Locatelli, V., Rigamonti, A.E., Torsello, A., Bresciani, E., Bulgarelli, I., Rizzi, R., Pavone, F., et al. (2006). TLQP-21, a VGF-derived peptide, increases energy expenditure and prevents the early phase of diet-induced obesity. Proc. Natl. Acad. Sci. USA *103*, 14584–14589.

Bérubé, N.G., Mangelsdorf, M., Jagla, M., Vanderluit, J., Garrick, D., Gibbons, R.J., Higgs, D.R., Slack, R.S., and Picketts, D.J. (2005). The chromatin-remodeling protein ATRX is critical for neuronal survival during corticogenesis. J. Clin. Invest. *115*, 258–267.

Bozdagi, O., Rich, E., Tronel, S., Sadahiro, M., Patterson, K., Shapiro, M.L., Alberini, C.M., Huntley, G.W., and Salton, S.R. (2008). The neurotrophin-inducible gene Vgf regulates hippocampal function and behavior through a

brain-derived neurotrophic factor-dependent mechanism. J. Neurosci. *28*, 9857–9869.

Brousse, B., Magalon, K., Durbec, P., and Cayre, M. (2015). Region and dynamic specificities of adult neural stem cells and oligodendrocyte precursors in myelin regeneration in the mouse brain. Biol. Open *4*, 980–992.

Chartier, C., Degryse, E., Gantzer, M., Dieterle, A., Pavirani, A., and Mehtali, M. (1996). Efficient generation of recombinant adenovirus vectors by homologous recombination in Escherichia coli. J. Virol. *70*, 4805–4810.

Chen, Y., Mei, R., Teng, P., Yang, A., Hu, X., Zhang, Z., Qiu, M., and Zhao, X. (2015). TAPP1 inhibits the differentiation of oligodendrocyte precursor cells via suppressing the Mek/Erk pathway. Neurosci. Bull. *31*, 517–526.

Colcombe, S.J., Kramer, A.F., McAuley, E., Erickson, K.I., and Scalf, P. (2004). Neurocognitive aging and cardiovascular fitness: recent findings and future directions. J. Mol. Neurosci. *24*, 9–14.

Cruise, K.E., Bucks, R.S., Loftus, A.M., Newton, R.U., Pegoraro, R., and Thomas, M.G. (2011). Exercise and Parkinson's: benefits for cognition and quality of life. Acta Neurol. Scand. *123*, 13–19.

Dadwal, P., Mahmud, N., Sinai, L., Azimi, A., Fatt, M., Wondisford, F.E., Miller, F.D., and Morshead, C.M. (2015). Activating endogenous neural precursor cells using metformin leads to neural repair and functional recovery in a model of childhood brain injury. Stem Cell Reports *5*, 166–173.

Dugas, J.C., Tai, Y.C., Speed, T.P., Ngai, J., and Barres, B.A. (2006). Functional genomic analysis of oligodendrocyte differentiation. J. Neurosci. *26*, 10967–10983.

Erickson, K.I., Voss, M.W., Prakash, R.S., Basak, C., Szabo, A., Chaddock, L., Kim, J.S., Heo, S., Alves, H., White, S.M., et al. (2011). Exercise training increases size of hippocampus and improves memory. Proc. Natl. Acad. Sci. USA *108*, 3017–3022.

Fernandes, A., Miller-Fleming, L., and Pais, T.F. (2014). Microglia and inflammation: conspiracy, controversy or control? Cell. Mol. Life Sci. *71*, 3969–3985.

Ferri, G.L., Noli, B., Brancia, C., D'Amato, F., and Cocco, C. (2011). VGF: an inducible gene product, precursor of a diverse array of neuro-endocrine peptides and tissue-specific disease biomarkers. J. Chem. Neuroanat. *42*, 249–261.

Fryer, J.D., Yu, P., Kang, H., Mandel-Brehm, C., Carter, A.N., Crespo-Barreto, J., Gao, Y., Flora, A., Shaw, C., Orr, H.T., and Zoghbi, H.Y. (2011). Exercise and genetic rescue of SCA1 via the transcriptional repressor Capicua. Science *334*, 690–693.

Gautier, H.O., Evans, K.A., Volbracht, K., James, R., Sitnikov, S., Lundgaard, I., James, F., Lao-Peregrin, C., Reynolds, R., Franklin, R.J., and Káradóttir, R.T. (2015). Neuronal activity regulates remyelination via glutamate signalling to oligodendrocyte progenitors. Nat. Commun. *6*, 8518.

Gibson, E.M., Purger, D., Mount, C.W., Goldstein, A.K., Lin, G.L., Wood, L.S., Inema, I., Miller, S.E., Bieri, G., Zuchero, J.B., et al. (2014). Neuronal activity promotes oligodendrogenesis and adaptive myelination in the mammalian brain. Science *344*, 1252304.

Hahm, S., Mizuno, T.M., Wu, T.J., Wisor, J.P., Priest, C.A., Kozak, C.A., Boozer, C.N., Peng, B., McEvoy, R.C., Good, P., et al. (1999). Targeted deletion of the Vgf gene indicates that the encoded secretory peptide precursor plays a novel role in the regulation of energy balance. Neuron *23*, 537–548.

Heyn, P., Abreu, B.C., and Ottenbacher, K.J. (2004). The effects of exercise training on elderly persons with cognitive impairment and dementia: a meta-analysis. Arch. Phys. Med. Rehabil. *85*, 1694–1704.

Hunsberger, J.G., Newton, S.S., Bennett, A.H., Duman, C.H., Russell, D.S., Salton, S.R., and Duman, R.S. (2007). Antidepressant actions of the exercise-regulated gene VGF. Nat. Med. *13*, 1476–1482.

Khalil, H., Quinn, L., van Deursen, R., Dawes, H., Playle, R., Rosser, A., and Busse, M. (2013). What effect does a structured home-based exercise programme have on people with Huntington's disease? A randomized, controlled pilot study. Clin. Rehabil. *27*, 646–658.

Kobilo, T., Yuan, C., and van Praag, H. (2011). Endurance factors improve hippocampal neurogenesis and spatial memory in mice. Learn. Mem. *18*, 103–107.

Krityakiarana, W., Espinosa-Jeffrey, A., Ghiani, C.A., Zhao, P.M., Topaldjikian, N., Gomez-Pinilla, F., Yamaguchi, M., Kotchabhakdi, N., and de Vellis, J. (2010). Voluntary exercise increases oligodendrogenesis in spinal cord. Int. J. Neurosci. *120*, 280–290.

Lewis, J.E., Brameld, J.M., and Jethwa, P.H. (2015). Neuroendocrine Role for VGF. Front. Endocrinol. (Lausanne) *6*, 3.

McCarthy, K.D., and de Vellis, J. (1980). Preparation of separate astroglial and oligodendroglial cell cultures from rat cerebral tissue. J. Cell Biol. *85*, 890–902.

Miyamoto, N., Maki, T., Shindo, A., Liang, A.C., Maeda, M., Egawa, N., Itoh, K., Lo, E.K., Lok, J., Ihara, M., and Arai, K. (2015). Astrocytes promote oligodendrogenesis after white matter damage via brain-derived neurotrophic factor. J. Neurosci. *35*, 14002–14008.

O'Meara, R.W., Ryan, S.D., Colognato, H., and Kothary, R. (2011). Derivation of enriched oligodendrocyte cultures and oligodendrocyte/neuron myelinating co-cultures from post-natal murine tissues. J. Vis. Exp. *54*, 3324.

Pasinetti, G.M., Ungar, L.H., Lange, D.J., Yemul, S., Deng, H., Yuan, X., Brown, R.H., Cudkowicz, M.E., Newhall, K., Peskind, E., et al. (2006). Identification of potential CSF biomarkers in ALS. Neurology *66*, 1218–1222.

Pedersen, B.K., and Febbraio, M.A. (2012). Muscles, exercise and obesity: skeletal muscle as a secretory organ. Nat. Rev. Endocrinol. *8*, 457–465.

Pedersen, B.K., Pedersen, M., Krabbe, K.S., Bruunsgaard, H., Matthews, V.B., and Febbraio, M.A. (2009). Role of exercise-induced brain-derived neurotrophic factor production in the regulation of energy homeostasis in mammals. Exp. Physiol. *94*, 1153–1160.

Pereira, A.C., Huddleston, D.E., Brickman, A.M., Sosunov, A.A., Hen, R., McKhann, G.M., Sloan, R., Gage, F.H., Brown, T.R., and Small, S.A. (2007). An in vivo correlate of exercise-induced neurogenesis in the adult dentate gyrus. Proc. Natl. Acad. Sci. USA *104*, 5638–5643.

Piao, J., Major, T., Auyeung, G., Policarpio, E., Menon, J., Droms, L., Gutin, P., Uryu, K., Tchieu, J., Soulet, D., and Tabar, V. (2015). Human embryonic stem cell-derived oligodendrocyte progenitors remyelinate the brain and rescue behavioral deficits following radiation. Cell Stem Cell *16*, 198–210.

Poulin, K.L., Lanthier, R.M., Smith, A.C., Christou, C., Risco Quiroz, M., Powell, K.L., O'Meara, R.W., Kothary, R., Lorimer, I.A., and Parks, R.J. (2010). Retargeting of adenovirus vectors through genetic fusion of a single-chain or single-domain antibody to capsid protein IX. J. Virol. *84*, 10074–10086.

Pysh, J.J., and Weiss, G.M. (1979). Exercise during development induces an increase in Purkinje cell dendritic tree size. Science *206*, 230–232.

Ross, P.J., and Parks, R.J. (2009). Construction and characterization of adenovirus vectors. Cold Spring Harb. Protoc. *4*, 1–12.

Selle, H., Lamerz, J., Buerger, K., Dessauer, A., Hager, K., Hampel, H., Karl, J., Kellmann, M., Lannfelt, L., Louhija, J., et al. (2005). Identification of novel biomarker candidates by differential peptidomics analysis of cerebrospinal fluid in Alzheimer's disease. Comb. Chem. High Throughput Screen. *8*, 801–806.

Severini, C., Ciotti, M.T., Biondini, L., Quaresima, S., Rinaldi, A.M., Levi, A., Frank, C., and Possenti, R. (2008). TLQP-21, a neuroendocrine VGF-derived peptide, prevents cerebellar granule cells death induced by serum and potassium deprivation. J. Neurochem. *104*, 534–544.

Shimazawa, M., Tanaka, H., Ito, Y., Morimoto, N., Tsuruma, K., Kadokura, M., Tamura, S., Inoue, T., Yamada, M., Takahashi, H., et al. (2010). An inducer of VGF protects cells against ER stress-induced cell death and prolongs survival in the mutant SOD1 animal models of familial ALS. PLoS ONE *5*, e15307.

Skaper, S.D. (2007). The brain as a target for inflammatory processes and neuroprotective strategies. Ann. N Y Acad. Sci. *1122*, 23–34.

Stopka, T., and Skoultchi, A.I. (2003). The ISWI ATPase Snf2h is required for early mouse development. Proc. Natl. Acad. Sci. USA *100*, 14097–14102.

Thakker-Varia, S., Krol, J.J., Nettleton, J., Bilimoria, P.M., Bangasser, D.A., Shors, T.J., Black, I.B., and Alder, J. (2007). The neuropeptide VGF produces antidepressant-like behavioral effects and enhances proliferation in the hippocampus. J. Neurosci. *27*, 12156–12167.

Thakker-Varia, S., Jean, Y.Y., Parikh, P., Sizer, C.F., Jernstedt Ayer, J., Parikh, A., Hyde, T.M., Buyske, S., and Alder, J. (2010). The neuropeptide VGF is

reduced in human bipolar postmortem brain and contributes to some of the behavioral and molecular effects of lithium. J. Neurosci. *30*, 9368–9380.

Thakker-Varia, S., Behnke, J., Doobin, D., Dalal, V., Thakkar, K., Khadim, F., Wilson, E., Palmieri, A., Antila, H., Rantamaki, T., and Alder, J. (2014). VGF (TLQP-62)-induced neurogenesis targets early phase neural progenitor cells in the adult hippocampus and requires glutamate and BDNF signaling. Stem Cell Res. (Amst.) *12*, 762–777.

van Praag, H., Christie, B.R., Sejnowski, T.J., and Gage, F.H. (1999a). Running enhances neurogenesis, learning, and long-term potentiation in mice. Proc. Natl. Acad. Sci. USA *96*, 13427–13431.

van Praag, H., Kempermann, G., and Gage, F.H. (1999b). Running increases cell proliferation and neurogenesis in the adult mouse dentate gyrus. Nat. Neurosci. *2*, 266–270.

van Praag, H., Shubert, T., Zhao, C., and Gage, F.H. (2005). Exercise enhances learning and hippocampal neurogenesis in aged mice. J. Neurosci. *25*, 8680–8685.

Verghese, J., Lipton, R.B., Katz, M.J., Hall, C.B., Derby, C.A., Kuslansky, G., Ambrose, A.F., Sliwinski, M., and Buschke, H. (2003). Leisure activities and the risk of dementia in the elderly. N. Engl. J. Med. *348*, 2508–2516.

Wake, H., Ortiz, F.C., Woo, D.H., Lee, P.R., Angulo, M.C., and Fields, R.D. (2015). Nonsynaptic junctions on myelinating glia promote preferential myelination of electrically active axons. Nat. Commun. *6*, 7844.

Wang, J., Gallagher, D., DeVito, L.M., Cancino, G.I., Tsui, D., He, L., Keller, G.M., Frankland, P.W., Kaplan, D.R., and Miller, F.D. (2012). Metformin activates an atypical PKC-CBP pathway to promote neurogenesis and enhance spatial memory formation. Cell Stem Cell *11*, 23–35.

Wegener, A., Deboux, C., Bachelin, C., Frah, M., Kerninon, C., Seilhean, D., Weider, M., Wegner, M., and Nait-Oumesmar, B. (2015). Gain of Olig2 function in oligodendrocyte progenitors promotes remyelination. Brain *138*, 120–135.

Zatorre, R.J., Fields, R.D., and Johansen-Berg, H. (2012). Plasticity in gray and white: neuroimaging changes in brain structure during learning. Nat. Neurosci. *15*, 528–536.

Zhao, Z., Lange, D.J., Ho, L., Bonini, S., Shao, B., Salton, S.R., Thomas, S., and Pasinetti, G.M. (2008). Vgf is a novel biomarker associated with muscle weakness in amyotrophic lateral sclerosis (ALS), with a potential role in disease pathogenesis. Int. J. Med. Sci. *5*, 92–99.

Zhao, C., Ma, D., Zawadzka, M., Fancy, S.P., Elis-Williams, L., Bouvier, G., Stockley, J.H., de Castro, G.M., Wang, B., Jacobs, S., et al. (2015). Sox2 sustains recruitment of oligodendrocyte progenitor cells following CNS demyelination and primes them for differentiation during remyelination. J. Neurosci. *35*, 11482–11499.